

## SOLUTION OF THE THREE DIMENSIONAL SOIL-STRUCTURE INTERACTION PROBLEM IN THE TIME DOMAIN

E. Bayo (I)

E. L. Wilson (II)

Presenting Author: E. L. Wilson

### SUMMARY

A general time domain finite element formulation and several efficient numerical techniques are combined to form a new method of analysis for the solution of three-dimensional soil-structure interaction problems. Factors such as structural embedment, arbitrary soil-profile, flexibility of the foundation, spatial variations of free field motions and interaction between two or more structures are all incorporated in the new formulation. For elastic systems the method becomes extremely efficient however its major advantage is its ability to be extended to account for nonlinear effects in the soil and structure.

### INTRODUCTION

Solutions to soil-structure interaction problems are commonly carried out in the frequency domain. This is so, among other reasons, firstly because this domain permits, through the use of frequency dependent impedance coefficients, the splitting of the problem into substructures that can be analyzed independently; and secondly, because most of the transmitting boundaries developed to account for the radiation of the energy through the limits of the finite element model, are frequency dependent.

So far these reasons have been powerful enough to inhibit the time domain as the effective environment for the solution of the soil-structure problem. However, frequency domain techniques can not solve true nonlinear soil and structural problems, and are computationally inefficient for three dimensional problems. The purpose of this paper is to present a time domain formulation and efficient numerical techniques that can solve the soil-structure interaction problem in three dimensions, and at the same time allow for the solution of true nonlinear problems, feasible only in the time domain.

The discussion begins with the formulation of the soil-structure interaction problem in the time domain, it continues with the numerical techniques that make the solution of the problem efficient, and ends with a numerical example that shows the accuracy achieved by the new method compared to a frequency domain solution.

### FORMULATION IN THE TIME DOMAIN

A given soil-structure interaction problem may be divided as shown in Figure 1 into a free field, and an interaction problem in which the input motion is defined at the nodes corresponding to the buried part of the structure (Ref 1). This partition of the complete problem has a main advantage in eliminating the scattering problem, and only requires that the structural

(I) Fellow of the 'Fundacion del Instituto Nacional de Industria'. Spain.  
Assistant Research Engineer. University of California. Berkeley.

(II) Professor of Civil Engineering. University of California. Berkeley.

properties, stiffness, mass and damping, at its embedded level be reduced by those of the soil at the same level. The total displacements may be divided into the interaction and the free field displacements as follows:

$$\mathbf{v}'_c = \begin{Bmatrix} v'_f \\ v'_g \\ v'_a \end{Bmatrix} \quad \text{and} \quad \tilde{\mathbf{v}}_c = \begin{Bmatrix} 0 \\ \tilde{v}_f \\ \tilde{v}_g \\ \tilde{v}_a \end{Bmatrix} \quad (1)$$

where  $v$  represent the motions at the structure,  $v_f$  at the buried part,  $v_a$  at the soil and  $v_g$  at the soil-structure interface. The notation used for the property matrices are:

$$\mathbf{m}_c = \begin{bmatrix} m & m_f & 0 & 0 \\ m_f^T & m_{ff} - \tilde{m}_{ff} & m_{fg} - \tilde{m}_{fg} & 0 \\ 0 & m_{gf} - \tilde{m}_{gf} & m_{gg} & 0 \\ 0 & 0 & 0 & 0 \end{bmatrix} \quad \tilde{\mathbf{m}}_c = \begin{bmatrix} 0 & 0 & 0 & 0 \\ 0 & \tilde{m}_{ff} & \tilde{m}_{fg} & 0 \\ 0 & \tilde{m}_{gf} & \tilde{m}_{gg} & \tilde{m}_{ga} \\ 0 & 0 & \tilde{m}_{ag} & \tilde{m}_{aa} \end{bmatrix} \quad (2)$$

and in the same manner for the stiffness and damping matrices. The free field equations (Figure 1b) are:

$$\begin{bmatrix} \tilde{\mathbf{m}}_c & \tilde{\mathbf{m}}_b \\ \tilde{\mathbf{m}}_b^T & \tilde{\mathbf{m}}_{bb} \end{bmatrix} \begin{Bmatrix} \tilde{\mathbf{v}}_c \\ \tilde{\mathbf{v}}_b \end{Bmatrix} + \begin{bmatrix} \tilde{\mathbf{c}}_c & \tilde{\mathbf{c}}_b \\ \tilde{\mathbf{c}}_b^T & \tilde{\mathbf{c}}_{bb} \end{bmatrix} \begin{Bmatrix} \tilde{\mathbf{v}}_c \\ \tilde{\mathbf{v}}_b \end{Bmatrix} + \begin{bmatrix} \tilde{\mathbf{k}}_c & \tilde{\mathbf{k}}_b \\ \tilde{\mathbf{k}}_b^T & \tilde{\mathbf{k}}_{bb} \end{bmatrix} \begin{Bmatrix} \tilde{\mathbf{v}}_c \\ \tilde{\mathbf{v}}_b \end{Bmatrix} = \begin{Bmatrix} 0 \\ 0 \end{Bmatrix} \quad (3)$$

The equations for the interaction problem (Figure 1c) are (Ref 1):

$$\left[ \tilde{\mathbf{m}}_c + \mathbf{m}_c \right] \dot{\tilde{\mathbf{v}}}'_c + \left[ \tilde{\mathbf{c}}_c + \mathbf{c}_c \right] \dot{\tilde{\mathbf{v}}}'_c + \left[ \tilde{\mathbf{k}}_c + \mathbf{k}_c \right] \tilde{\mathbf{v}}'_c = -\mathbf{m}_c \tilde{\mathbf{v}}_c - \mathbf{c}_c \tilde{\mathbf{v}}_c - \mathbf{k}_c \tilde{\mathbf{v}}_c \quad (4)$$

The substitution of Equations (1) and (2) in Equation (4) yields:

$$\begin{bmatrix} \tilde{\mathbf{m}}_c + \mathbf{m}_c \end{bmatrix} \dot{\tilde{\mathbf{v}}}'_c + \begin{bmatrix} \tilde{\mathbf{c}}_c + \mathbf{c}_c \end{bmatrix} \dot{\tilde{\mathbf{v}}}'_c + \begin{bmatrix} \tilde{\mathbf{k}}_c + \mathbf{k}_c \end{bmatrix} \tilde{\mathbf{v}}'_c = - \begin{bmatrix} m_f & 0 \\ m_{ff} - \tilde{m}_{ff} & m_{fg} - \tilde{m}_{fg} \\ m_{gf} - \tilde{m}_{gf} & m_{gg} \\ 0 & 0 \end{bmatrix} \begin{Bmatrix} \tilde{v}_f \\ \tilde{v}_g \end{Bmatrix} - \begin{bmatrix} c_f & 0 \\ c_{ff} - \tilde{c}_{ff} & c_{gf} - \tilde{c}_{gf} \\ c_{gf} - \tilde{c}_{gf} & c_{gg} \\ 0 & 0 \end{bmatrix} \begin{Bmatrix} \tilde{v}_f \\ \tilde{v}_g \end{Bmatrix} - \begin{bmatrix} k_f & 0 \\ k_{ff} - \tilde{k}_{ff} & k_{fg} - \tilde{k}_{fg} \\ k_{gf} - \tilde{k}_{gf} & k_{gg} \\ 0 & 0 \end{bmatrix} \begin{Bmatrix} \tilde{v}_f \\ \tilde{v}_g \end{Bmatrix} \quad (5)$$

To simplify the notation let the matrices on the R.H.S. be called,  $\mathbf{X}_m$ ,  $\mathbf{X}_c$ , and  $\mathbf{X}_k$  respectively. The free field motions at the embedded nodes (Figure 1b) may be obtained by solving Equation (3) by assuming a desired wave propagation pattern. The simplest pattern is to assume vertical propagation of P and S waves. Equation (5) may be further simplified by dividing the added displacements in two parts: a dynamic component,  $\mathbf{v}_c$ , plus a pseudostatic component,  $\mathbf{v}_c^s$ , (Ref 2). The pseudostatic displacements may be derived from Equation (5) by eliminating the dynamic terms. The displacement decomposition is given by the following expression:

$$\mathbf{v}'_c = \mathbf{v}_c + \mathbf{v}_c^s = \mathbf{v}_c + \mathbf{r}_c \begin{Bmatrix} \tilde{v}_f \\ \tilde{v}_g \end{Bmatrix} \quad (6)$$

where:

$$\mathbf{r}_c = - \left[ \tilde{\mathbf{k}}_c + \mathbf{k}_c \right]^{-1} \begin{pmatrix} k_f & 0 \\ k_{ff} - \tilde{k}_{ff} & k_{fg} - \tilde{k}_{fg} \\ k_{gf} - \tilde{k}_{gf} & k_{gg} \\ 0 & 0 \end{pmatrix} \quad (7)$$

substituting Equations (6) and (7) into Equation (5):

$$\left[ \tilde{\mathbf{m}}_c + \mathbf{m}_c \right] \ddot{\mathbf{v}}_c + \left[ \tilde{\mathbf{c}}_c + \mathbf{c}_c \right] \dot{\mathbf{v}}_c + \left[ \tilde{\mathbf{k}}_c + \mathbf{k}_c \right] \mathbf{v}_c = \left\{ \left[ \tilde{\mathbf{m}}_c + \mathbf{m}_c \right] \mathbf{r}_c + \mathbf{X}_m \right\} \begin{pmatrix} \hat{v}_f \\ \hat{v}_g \end{pmatrix} \quad (8)$$

Equation (8) defines the motion of the system in terms of the dynamic displacements, and as a function of the free field ground motions at the buried part of the structure. It is easily seen that the forces in the nonburied part of the structure will depend only on the dynamic displacements, whereas, those in the buried part will now depend on the dynamic as well as on the free field displacements. The nonlinear problem can be solved by dividing the system, as shown in Figure 2, into a scattering and an interaction problem. The interaction motions contain the total displacements of the structure and the nonlinear part of the soil, therefore Equation (4) is suitable for nonlinear analysis in those regions.

#### REDUCTION OF THE SYSTEM OF EQUATIONS

The authors have demonstrated (Ref 3) that the use of sets of a special class of Ritz vectors (Ref 4) lead to very good solutions for wave propagation and structure-soil interaction problems. Several ways of using them as part of dynamic substructuring techniques have also been shown (Ref.1,3). The reduction in the size of the given problem can be done using those substructuring techniques, however, for simplicity in this discussion we will use the Ritz vectors globally, without making use of any substructuring procedure. Let the following displacement transformation be defined:

$$\begin{pmatrix} v \\ v_f \\ v_g \\ v_a \end{pmatrix} = \Phi \mathbf{Y} \quad (9)$$

where  $\Phi$  are the global Ritz vectors and  $\mathbf{Y}$  are the generalized coordinates. The substitution of the above transformation into Equation (8), and the premultiplication by  $\Phi^T$ , leads to:

$$\mathbf{M}^* \ddot{\mathbf{Y}} + \mathbf{C}^* \dot{\mathbf{Y}} + \mathbf{K}^* \mathbf{Y} = -\Phi^T \left\{ \left[ \tilde{\mathbf{m}}_c + \mathbf{m}_c \right] \mathbf{r}_c + \mathbf{X}_m \right\} \begin{pmatrix} \hat{v}_f \\ \hat{v}_g \end{pmatrix} \quad (10)$$

where

$$\mathbf{M}^* = \Phi^T \left[ \mathbf{m}_c + \tilde{\mathbf{m}}_c \right] \Phi \quad \mathbf{C}^* = \Phi^T \left[ \mathbf{c}_c + \tilde{\mathbf{c}}_c \right] \Phi \quad \mathbf{K}^* = \Phi^T \left[ \mathbf{k}_c + \tilde{\mathbf{k}}_c \right] \Phi \quad (11)$$

The numerical integration of the reduced coupled set of equations can be carried out by step-by-step procedures or by decoupling the system with complex eigenvectors, and solving each of the uncoupled equations by the linear force method. The second approach becomes exact for piece-wise linear type of excitation, while the first always introduces errors in the amplitude and periods of the response. For reduced systems of equations (up to 100 mode shapes) the complex eigenvector method is as computationally efficient as the step-by-step methods, and therefore it becomes a better candidate for numerical integration (Ref 1).

### MODELING THE SOIL-STRUCTURE SYSTEM

The size of a typical three dimensional soil-structure interaction problem will in general be very large. The use of approximate frequency independent boundaries (Ref 5) still requires moderate sizes of finite element models. In order to further reduce the size of the problem a technique for geometrically modeling the soil-structure system is described below. This technique is based on the combined use of solid and axisymmetric elements to model the near and far field respectively. The reason behind this approach is that the behaviour of the soil system in the far field, away from the structure, will tend to be that of an axisymmetric system subjected to non-axisymmetric loads.

Figure 3 shows a method of modeling a soil-structure system. A given structure will be represented with standard finite elements. The foundation will be attached to the near field part of the soil, that is modeled with solid elements. At a certain distance from the structure the solid mesh is attached to the far field that is modeled by means of several harmonic expansions of axisymmetric finite elements. In order to couple both the near and the far fields, the displacements corresponding to the solid elements at the boundary between both regions are expanded in terms of Fourier series. The corresponding displacement transformation matrices (Ref 1), are used to transform the solid mass, stiffness, and damping matrices of the solid elements in contact with the axisymmetric mesh.

Another aspect to consider in modeling the soil-structure system is the internal damping. The damping characteristics of each of the components, soil and structure, can be independently represented by the Rayleigh damping model defined from damping ratios at two different frequencies. Damping ratios for soils are usually kept constant over all the frequency range. A good selection of the frequencies necessary to define the Rayleigh damping model will keep the variation of the damping ratio quite constant over a wide frequency interval, as will be seen in the numerical case given below. For cases where the frequency range of interest is too large several terms of the Caughey series can be considered to maintain a constant damping ratio (Ref 1). Since different damping ratios are considered for the soil and the structure, the resulting global damping matrix will be nonproportional. The consideration of a transmitting boundary will further contribute to the nonproportionality of the damping matrix.

### NUMERICAL EXAMPLE

The procedures explained above have been implemented in a special version of the computer program SAP80 (Ref 6) for the solution of soil-structure interaction problems. To evaluate their effectiveness, a three dimensional soil structure system, whose characteristics are shown in Figure 4, is analyzed. The superstructure consists of a 2 degree of freedom system attached to a rigid massless circular foundation. The lumped masses are connected by frame

elements. The foundation is attached to a semi-infinite half-space with the characteristics depicted in Figure 4. The half-space is discretized with axisymmetric finite elements. The length and depth of the model are 5.5 and 5.8 times the radius respectively, with a total number of degrees of freedom equal to 714. The material damping is assigned a constant value for all the frequency range equal to 7 %. In order to represent this behaviour in the time domain the Rayleigh damping model is used. The frequencies taken to match the given damping ratio are 23 and 70 rd/sec. This will insure a variation of the damping ratio of less than 0.9% (ie. 6.1 to 7.9 %) over the frequency range of  $21 < \omega < 87$  rd/sec. This corroborates the fact that Rayleigh damping models can provide a quite constant damping ratio over a wide range of frequencies. Attached to the edges of the model there is a frequency independent transmitting boundary defined at the fundamental frequency of the system (Ref 5) which has been previously computed to be 25.8 rd/sec.

The frequencies of the 2 degree of freedom model on a fixed base are 34.24 and 85.38 rd/sec. The significance of the soil-structure interaction effects in the dynamic response of the system is apparent from the fact that the first resonant frequency for the structural response has been reduced from 34.24 to 25.80 rd/sec. The second resonant frequency varies to a lesser degree from 85.38 to 80.42 rd/sec. The total system of equations is reduced globally, as explained above, with 2 different sets of Ritz vectors, the first one has 15 Ritz functions and the second 40 (2.1 and 5.6 % of the total number of degrees of freedom respectively). By running these two cases the convergence of the Ritz vector approach can be checked. The system is to be subjected to the vertical component of an earthquake excitation represented by the first 8 seconds of a given accelerogram, discretized at time intervals of 0.01 seconds and with peak acceleration equal to 0.26 g. The results obtained with SAP80 are to be compared with those obtained by the computer program SASSI (Ref 7). SASSI solves the problem using a frequency domain formulation. It uses frequency dependent radiation boundaries, and complex stiffness coefficients to account for the constant damping ratio.

The structure-soil model is solved first by SAP80, with 15 Ritz functions and with numerical integration by the complex eigenvectors, and second by SASSI. The total maximum accelerations in "g" obtained by both programs are given in Table 1. The maximum discrepancy is 3.6%. Figure 5 shows the response spectrum at degree of freedom 1 for 5% damping. As can be seen both solutions are very close. The discrepancy between the two solutions at the peak of the spectrum is 9%.

The total maximum accelerations at both degrees of freedom obtained by SAP80 with 40 Ritz functions, and SASSI are given in Table 2. The maximum discrepancy is now 2.5%. The response spectrum at degree of freedom 1 for 5% damping is shown in Figure 6, and indicates how close both solutions are. The differences in the interval of periods between 0.2 and 0.3 seconds are due to the different ways in which both methods represent the material damping. The maximum discrepancy at the peak is now 2.5%.

PROGRAM	DOF1	DOF2
SASSI	-0.440	-0.393
SAP80	-0.456	-0.402

Table 1.

PROGRAM	DOF1	DOF2
SASSI	-0.440	-0.393
SAP80	-0.452	-0.400

Table 2.

In order to see how important the interaction effects are in this case,

the two degree of freedom model is analyzed for the given input considering its base fixed. The maximum accelerations obtained in this way are 0.647 g and 0.424 g, which indicates that the reduction achieved by considering the interaction between soil and structure is of the order of 30%. This difference increases substantially when comparing the response spectrum of the model with and without interaction effects, as illustrated in Figure 7. It shows the drastic reduction of the response and the shifting of the resonant periods due to the interaction. A third resonant period appears at 0.29 seconds due to the participation of the soil.

Another aspect worth of analysis is the importance that the transmitting boundaries have in the response of the system. For this purpose the same example is solved again using 15 Ritz functions, with the bottom boundary fixed and allowing horizontal displacements at the lateral boundaries. Figure 8 illustrates the response spectrum obtained under these conditions compared with those obtained previously, which included the transmitting boundaries. As can be seen the errors introduced by not including transmitting boundaries in the finite element model are considerable, even for an input of short duration as in this case (only 8 seconds).

#### REFERENCES

- 1 Bayo, E. and Wilson, E. L. "Numerical Techniques for the Evaluation of Soil-Structure Interaction Effects in the Time Domain". EERC report 83/04. University of California. Berkeley. California. Feb 1983.
- 2 Clough, R.W., and Penzien, J. "Dynamic of Structures." McGraw-Hill, (1975).
- 3 Bayo, E. and Wilson, E. L. "Use of Ritz Vectors in Wave Propagation and Dynamic Substructuring Analysis". Earth. Eng. Struct. Dynam. Submitted for Publication.
- 4 Wilson, E.L., Yuan, M-W, Dickens J.M. "Dynamic Analysis by Direct Superposition of Ritz Vectors". Earth. Eng. Struc. Dynam. Vol 10. pp 813-823 (1982).
- 5 Bayo, E. and Wilson, E. L. "Transmitting Boundaries for Transient Dynamic Analysis". Earth. Eng. Struct. Dynam. Submitted for Publication.
- 6 Wilson, E. L. "SAP80 Structural Analysis Programs for Small or Large Computer Systems". CEPA 1980 Fall Conference and Annual Meeting. Newport Beach. California.
- 7 Lysmer J., Raissi, M., Tajirian, F., Vahdani, S., Ostandan, F. "SASSI- A System For Analysis of Soil-Structure Interaction". University of California Berkeley. Geotechnical report # 81-02. April (1981).

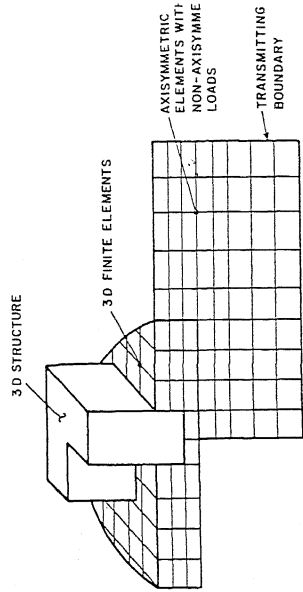
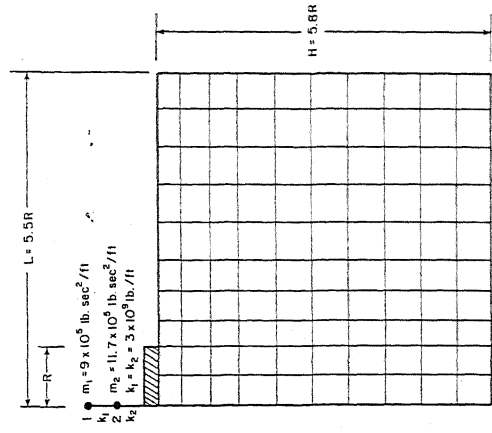


Fig 3.- Modeling soil-structure problems.



$V_p = 4000 \text{ ft/sec}$   
 $\nu = 1/3$   
 $G = 1.244 \times 10^7 \text{ lb/ft}^2$   
 $V_t = 2000 \text{ ft/sec}$   
 $P = 3.11 \text{ lb. sec}^2/\text{ft}^4$   
 $E = 3.17 \times 10^7 \text{ lb/ft}^2$   
 $R = 42 \text{ ft}$

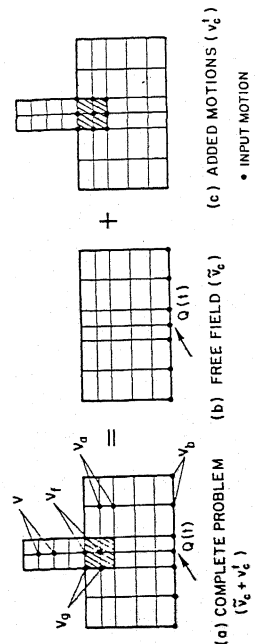


Fig 1.- Division of the complete problem into a free field and an interaction problem.

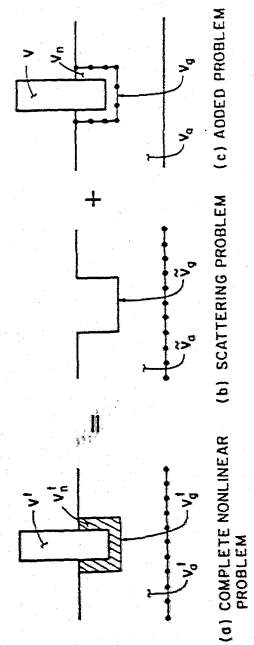


Fig 4.- Characteristics of the numerical example.

Fig 2.- Two step solution for the nonlinear problem.

DEGREE OF FREEDOM 1 RESPONSE SPECTRUM 5% DAMPING

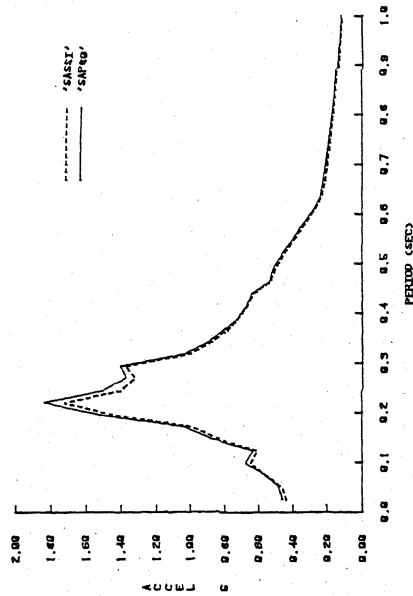


Fig 5.- Response spectrum at DOF1 obtained with SAP80 using 15 Ritz functions, and SASSI.

DEGREE OF FREEDOM 1 RESPONSE SPECTRUM 5% DAMPING

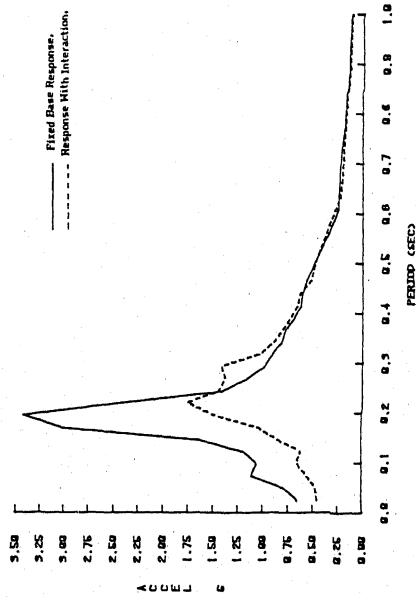


Fig 7.- Response spectrum at DOF1 obtained with end without interaction effects.

DEGREE OF FREEDOM 1 RESPONSE SPECTRUM 5% DAMPING

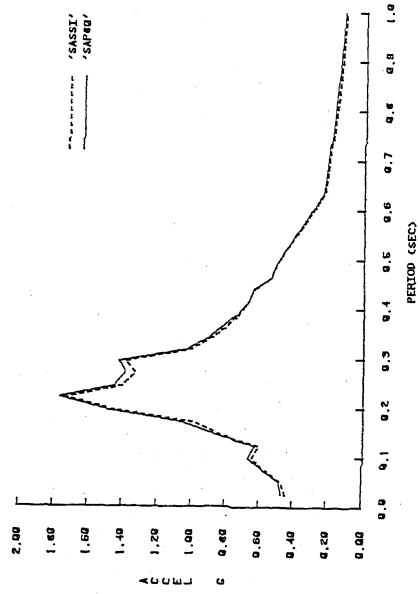


Fig 6.- Response spectrum at DOF1 obtained with SAP80 using 40 Ritz functions, and SASSI.

DEGREE OF FREEDOM 1 RESPONSE SPECTRUM 5% DAMPING

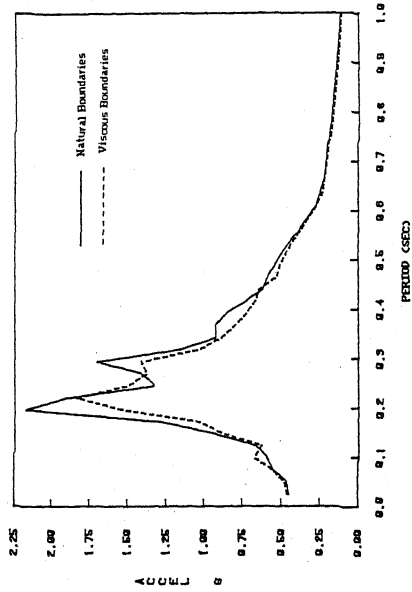


Fig 8.- Response spectrum at DOF1 obtained with end without transmitting boundaries.